Vision Research 50 (2010) 2396–2402

Contents lists available at ScienceDirect

Vision Research

journal homepage: www.elsevier.com/locate/visres

Color-deficient cone mosaics associated with Xq28 opsin mutations: A stop codon versus gene deletions

Melissa Wagner-Schuman [a], Jay Neitz [b], Jungtae Rha [c], David R. Williams [d], Maureen Neitz [b], Joseph Carroll [a,c,e,*]

[a] Department of Biophysics, Medical College of Wisconsin, Milwaukee, WI 53226, United States
[b] Department of Ophthalmology, University of Washington Medical School, Seattle, WA 98195, United States
[c] Department of Ophthalmology, Medical College of Wisconsin, Milwaukee, WI 53226, United States
[d] Center for Visual Science, University of Rochester, Rochester, NY 14627, United States
[e] Department of Cell Biology, Neurobiology, & Anatomy, Medical College of Wisconsin, Milwaukee, WI 53226, United States

ARTICLE INFO

Article history:
Received 17 May 2010
Received in revised form 10 September 2010

Keywords:
Adaptive optics
Color vision
Cones
Deutan
Opsin gene

ABSTRACT

Our understanding of the etiology of red–green color vision defects is evolving. While missense mutations within the long- (L-) and middle-wavelength sensitive (M-) photopigments and gross rearrangements within the L/M-opsin gene array are commonly associated with red–green defects, recent work using adaptive optics retinal imaging has shown that different genotypes can have distinct consequences for the cone mosaic. Here we examined the cone mosaic in red–green color deficient individuals with multiple X-chromosome opsin genes that encode L opsin, as well as individuals with a single X-chromosome opsin gene that encodes L opsin and a single patient with a novel premature termination codon in his M-opsin gene and a normal L-opsin gene. We observed no difference in cone density between normal trichomats and multiple or single-gene deutans. In addition, we demonstrate different phenotypic effects of a nonsense mutation versus the previously described deleterious polymorphism, (LIAVA), both of which differ from multiple and single-gene deutans. Our results help refine the relationship between opsin genotype and cone photoreceptor mosaic phenotype.

1. Introduction

Unequal homologous recombination produces rearrangements of the array of long- (L) and middle-wavelength sensitive (M-) cone opsin genes on the X-chromosome; these rearrangements are the most common cause of inherited red–green color vision deficiency (Drummond-Borg, Deeb, & Motolsky, 1989; Nathans, Thomas, & Hogness, 1986). In individuals with inherited red–green color vision defects there is tremendous variation in both the arrangement of cone opsin genes and in the associated color vision phenotype (Bollinger, Bialozynski, Neitz, & Neitz, 2001; Deeb et al., 1992; Jagla, Jägle, Hayashi, Sharpe, & Deeb, 2002; Nathans et al., 1986; Neitz et al., 2004; Sharpe et al., 1998; Ueyama et al., 2004). Over the past 25 years great strides have been made in understanding how the nature of the gene rearrangements affects phenotype in terms of color vision behavior. Recently, high-resolution imaging of the cone mosaic in the living human eye using adaptive optics has made it possible to address the question of how different genetic rearrangements affect the retinal phenotype at the cellular level.

The most common color vision deficiencies are deutan defects, which are characterized by a loss of M-cone function and often associated with X-chromosome opsin gene arrays in which the first two head-to-tail genes at the 5′-end of the array encode L opsin. If the encoded opsins form pigments that differ in spectral sensitivity, the resulting behavioral phenotype is deuteranomalous trichromacy, but if they form pigments of identical spectra the behavioral phenotype is deuteranopia. In arrays with more than two opsin genes, only the first two are usually expressed, so the additional downstream genes will not affect the color vision phenotype (Hayashi, Motulsky, & Deeb, 1999; Neitz, Bollinger, & Neitz, 2003). Deuteranopic defects will also occur when all but one of the X-chromosome opsin genes is deleted, leaving an array that contains one functional L-opsin gene (Nathans et al., 1986; Neitz et al., 2004). It is unknown whether or how the cellular phenotype varies between single- and multiple-gene deutans.

More rarely, mutations that ultimately render the opsin or photopigment non-functional have also been identified as a cause of inherited red–green color vision deficiencies. These mutations fall into two categories. The first category encompasses a variety of missense mutations that are the result of random mutations that

* Corresponding author. Address: The Eye Institute, 925 N. 87th Street, Milwaukee, WI 53226, United States. Fax: +1 414 456 6690.
E-mail address: jcarroll@mcw.edu (J. Carroll).

0042-6989/$ - see front matter © 2010 Elsevier Ltd. All rights reserved.
doi:10.1016/j.visres.2010.09.015

introduce a nucleotide change that creates a deleterious amino acid substitution (Gardner et al., 2010; Neitz et al., 2004; Ueyama et al., 2002; Winderickx et al., 1992). The most common of these is the replacement of the highly conserved cysteine residue at position 203 with arginine (C203R) (Bollinger, Bialozynski, Jagla et al., 2002; Neitz & Neitz, 2001; Neitz et al., 2004; Winderickx et al., 1992). The second category has only recently been recognized, and includes deleterious combinations of amino acids at dimorphic positions that distinguish ancestral L from M opsins. These combinations appear to have arisen via recombination events that mix L and M genes together, producing new alleles that encode pigments that ultimately lead to photoreceptor dysfunction. Three such combinations involving amino acids encoded by exon 3 are leucine 153, isoleucine 171, alanine 174, valine 178, and alanine 180, abbreviated "LIAVA" using the single letter amino acid code (Carroll, Neitz, Hofer, Neitz, & Williams, 2004; Neitz et al., 2004), leucine 153, isoleucine 171, alanine 174, valine 178, and serine 180, abbreviated "LIAVS" (Mizrahi-Meissonnier, Merin, Banin, & Sharon, 2010), and leucine 153, valine 171, alanine 174, valine 178, and alanine 180, abbreviated "LVAVA" (McClements, Neitz, Moore, & Hunt, 2010). Adaptive optics imaging has been used to investigate the effect of the C203R mutation and the LIAVA polymorphism on the architecture of the cone mosaic in terms of cone density and cone packing in individuals with a red–green color vision defect (Carroll et al., 2004, 2009; Torti et al., 2009). For two individuals with the C203R mutation and one individual with the LIAVA polymorphism, adaptive optics revealed reduced cone densities compared to normal trichromats (Carroll et al., 2009; Torti et al., 2009). For the LIAVA polymorphism, the appearance of the cone mosaic suggested that the LIAVA-encoding M-opsin gene was expressed in a subset of cones that became nonfunctional at some point after foveal cone migration had completed, leaving areas where no cones were visible in the adaptive optics images (Carroll et al., 2004). In contrast, the appearance of the retinas with the C203R mutation suggests that cones were lost prior to the completion of foveal cone migration. This would result in a contiguous cone mosaic, albeit of overall reduced density (Carroll et al., 2009). Understanding how additional mutations affect the health of the cone photoreceptor mosaic at the cellular level would help establish a more comprehensive understanding of the etiology of red–green color vision defects.

We identified a patient with a novel missense mutation in his M-opsin gene at codon 149 that changes it from coding for the amino acid tryptophan (W) to a translation termination signal (X). There is no known equivalent rhodopsin mutation at this location. This mutation adds to the growing number of missense mutations reported in the L/M opsins; at least eleven other missense mutations have been reported: C203R (Winderickx et al., 1992), R247X and P307L (Nathans et al., 1993), N94K, R330Q, and G338E (Ueyama et al., 2002), P231L (Ueyama et al., 2004), P187L (Neitz et al., 2004), W90X (Wissinger, Papke, Tippmann, & Kohl, 2006), V120M (Mizrahi-Meissonnier et al., 2010) and W177R (Gardner et al., 2010). Of these missense mutations only W90X, reported by Wissinger et al. (2006) in a single patient with blue cone monochromacy, results in a translation termination signal. Here we used adaptive optics imaging to evaluate the cone mosaic in our patient with the M-opsin gene mutation in codon 149 (W149X). In addition, we assessed cone density and cone mosaic regularity for 9 other deutans, four with multiple-gene arrays and five with single-gene arrays. Individuals with multiple-gene arrays would be expected to have cone mosaics with similar density and regularity as mosaics from normal trichromats because, just as for a normal trichromat, the first two genes in the array are expressed in separate populations of cones (Bollinger, Sjoberg, Neitz, & Neitz, 2004). X-chromosome opsin gene arrays with a single gene can be considered as equivalent to an opsin gene knockout. A single transcriptional enhancer is shared by all opsin genes in the array, ensuring mutually exclusive expression (Smallwood, Wang, & Nathans, 2002), so it is anticipated that all of the cones destined to be L or M cones would express the available X-chromosome opsin gene in a single-gene deutan. If true, the cone mosaics of single-gene deutans might be expected to be indistinguishable from those of normal trichromats and of multiple-gene deutans. However, if cones that would have normally expressed the second gene in the array do not express any opsin gene, then we might expect a reduction in cone density owing to the absence of opsin (Carroll et al., 2010). In the case of the W149X mutation, the mutant opsin gene should be transcribed, at least initially; however, mammalian cells have "surveillance" mechanisms that maintain tight quality control on the biogenesis of messenger RNA (mRNA), including one that promotes rapid decay of mRNAs containing a premature translation termination codon in all but the last exon. This ultimately leads to down regulation of transcription of the mutant gene (Silva & Romano, 2009). Thus, the W149X mutant cone opsin would be expected to give rise to cones that neither contain a photopigment nor elaborate an outer segment.

Our imaging results revealed no significant difference in cone density or regularity between the single-gene deutans and the multiple-gene deutans or normal trichromats, providing the first direct evidence that individuals whose opsin gene arrays have been reduced to a single gene have complete retinal cone mosaics. In addition, the W149X mutation was associated with a reduced cone density, consistent with cone opsin playing an important structural role for the cone photoreceptor.

2. Methods

2.1. Subjects

Individuals with normal color vision as well as individuals with color vision defects were recruited by advertisement and most were of Western European ancestry. Ten deutans (nine males, one female; ranging in age from 10 to 55, with a mean of 29 years) and 27 normal trichromats (18 females, nine males; ranging in age from 10 to 55, with a mean of 26 years) were identified and recruited for adaptive optics retinal imaging. A complete ophthalmic exam was performed on the individual whose deutan color vision defect was caused by a novel opsin mutation, subject 6643 (age 40 years), which included visual acuity measurement, autofluorescence imaging, and dilated funduscopic exam. This examination was unremarkable and subject 6643 had a best-corrected visual acuity of 20/20. Axial length was measured on all subjects using a Zeiss IOLMaster (Carl Zeiss Meditec, Dublin, CA) for calibration of adaptive optics images. All research on human subjects followed the tenets of the Declaration of Helsinki and was approved by IRBs at the Medical College of Wisconsin (genetics, color-vision testing, and adaptive optics imaging) and the University of Rochester (color-vision testing and adaptive optics imaging). Informed consent was obtained from all participating adults as well as from parents of participating minors, after explanation of the nature and possible consequences of the study.

2.2. Color-vision testing

Color vision was assessed using the Neitz Test of Color Vision (Neitz & Neitz, 2001) and those whose performance indicated a red–green deficit were examined further using a variety of color vision tests including the AO-HRR, the Farnsworth-Munsell 100-Hue Test, the Lanthony's Desturated D-15, and Rayleigh color match on a Nagel Model 1 anomaloscope (Schmidt Haensch). Individuals who manifested a protan defect on all tests were excluded from the current study.

2.3. Genetic analyses

Genetic testing was performed on the subjects with a color vision deficiency. Genomic DNA was isolated from whole blood and used in the polymerase chain reaction to selectively amplify L and M genes. The resulting PCR products were used to amplify separately exons 2–4 of each gene, which were directly sequenced. The primers and thermal cycling parameters for all amplifications and for DNA sequencing have been previously reported (Neitz et al., 2004). Two previously described real-time quantitative polymerase chain reaction assays (Neitz & Neitz, 2001) were used to estimate the relative percentage of opsin genes on the X-chromosome that are downstream of the first gene in the array and the relative percentage of L versus M genes. Each estimate was based on the average of quadruplicate reactions.

2.4. Adaptive optics imaging

Images of the cone mosaics were obtained for 10 deutans and 27 normal controls using either the Rochester Second Generation Adaptive Optics System (Hofer et al., 2001) or the Medical College of Wisconsin Adaptive Optics System (Rha, Schroeder, Godara, & Carroll, 2009). For both systems, the head was stabilized using a dental impression on a bite bar. Each subjects' right eye was dilated and accommodation suspended through use of phenylephrine hydrochloride (2.5%) and tropicamide (1%). A series of retinal locations was imaged, using a paper fixation target as guide for the relative location (direction and eccentricity) of each image. These locations were recorded and the images at each location were analyzed separately to assess density and spatial organization of the cone mosaic.

2.5. Adaptive optics image analysis

Cone density and mosaic regularity were evaluated using a modified version of previously described automated Matlab (Mathworks, Natick, MA) software (Baraas et al., 2007; Li & Roorda, 2007). Key changes included an objective setting of the spatial filter and the ability for the user to manually adjust any of the automatically identified cone locations. Images from between one and five retinal locations (0.5°, 0.75°, 1.0°, 1.25°, and/or 2.5°) were analyzed to assess mosaic regularity in normal trichromats, single and multiple-gene deutans, and a deutan with a premature termination codon mutation. Metrics used to assess spatial organization included the average and standard deviation of intercone distances as well as the characteristics of Voronoi domains, specifically the Voronoi area and number of six-sided Voronoi domains. Voronoi analysis was completed via identification of each cone as a point in the retinal image. Subsequently, for each cone, a Voronoi boundary was constructed by defining the points in a 2D plane that were equidistant between that cone and each of its nearest neighbors. This results in the construction of a polygon (the Voronoi domain) for each cone. The more triangularly packed the mosaic, the more cones with six-sided Voronoi domains and six neighboring cones; this was used as a measure of the regularity of the retinal mosaic. Intercone distance and Voronoi area were also used as indicators of the photoreceptor packing regularity.

3. Results

3.1. Color-vision testing

Ten subjects were identified as having a red–green color vision defect based on results from the Neitz Test of Color Vision. Results from a variety of additional color vision tests classified subjects 400, 3503, 3507, 3511, 3513, 6643, and 6760 as deuteranopes while the remaining three subjects (433, 3509, 6537) were classified as deuteranomalous trichromats (Table 1).

3.2. Genetic results

Molecular genetic data for the ten deutan subjects are summarized in Table 1. Real-time quantitative PCR results revealed an estimate of 100% L genes and 0% downstream genes for five subjects (3503, 3507, 3511, 3513, and 6760). An estimate of 0% downstream genes is interpreted as there being one opsin gene on the X-chromosome. Deutan subjects with 0% downstream genes and 100% L genes are interpreted as having one X-chromosome ospin gene, and it encodes an L opsin. Four subjects (400, 433, 3509, and 6537) were estimated to have ~50% or ~66% downstream genes which is interpreted as there being two or three opsin genes on the X-chromosome, respectively. Those with ~50% L and ~50% downstream genes were interpreted as having 1L and 1M gene, those with ~66% L and ~66% downstream were interpreted to have 2L and 1M gene, and those with ~50% L and ~75% downstream genes were interpreted as having 2L and 2M genes. One deutan subject, 6643, was estimated to have ~50% L and ~50% downstream genes, which is interpreted as his having one L and one M gene. Sequencing results for this subject revealed a single nucleotide substitution in exon 3 of the M-opsin gene that creates a W149X mutation in which codon 149 is changed from TGG, which specifies the amino acid tryptophan (W), to TAG which specifies a translational stop signal (X) as shown in Fig. 1.

3.3. Imaging results

Adaptive optics retinal images were obtained from the 37 subjects enrolled in this study. Subjects were separated into three groups based on their color vision phenotype and genotype; single-gene deutans, multiple-gene deutans, and normal trichromats. Subject 6643, who was behaviorally classified as a deutan and identified as having a W149X mutation encoded by his M-opsin gene, was analyzed separately.

3.3.1. Parafoveal cone density

We determined cone density at up to five retinal locations for each subjects (0.5°, 0.75°, 1°, 1.25°, and/or 2.5° of retinal eccentricity). Raw data are provided in Supplemental Tables 1 and 2. The mean cone densities for each of the five retinal locations are plotted in Fig. 2, along with cone densities for the subject with the W149X mutation. A Z-score analysis revealed a significant reduction in cone density for the subject with the W149X mutation compared to normal trichromats with p values as follows: 0.5° $p = 0.062$; 0.75° $p = 0.027$; 1.0° $p = 0.016$; 1.25° $p = 0.029$; 2.5° $p = 0.015$. On average, across the five retinal eccentricities, subject 6643 had a cone density that was 32% lower than the mean density for the normal trichromats. The mean cone densities between the normal trichromats, single-gene deutans, and multiple-gene deutans were not significantly different from each other at any of the locations measured (ANOVA plus Bonferroni multiple comparison, $p > 0.17$), and were consistent with average cone densities reported from histological analysis (Curcio, Sloan, Kalina, & Hendrickson, 1990). Cone densities were highly variable within each group, consistent with previous adaptive optics reports evaluating cone density near the fovea (Carroll et al., 2010; Chui, Song, & Burns, 2008; Duncan et al., 2007; Li, Tiruveedhula, & Roorda, 2010; Putnam et al., 2005).

3.3.2. Cone photoreceptor mosaic regularity

In order to visualize the impact of the nonsense mutation on the regularity of the cone mosaic we employed a Voronoi analysis. Representative adaptive optics images taken from approximately

Table 1
Genetic and color vision results.

Genotypic group	Subject ID	% L genes	% Downstream genes	No. L genes	No. M genes	M gene mutation	AO-HRR[b]	D-15[c]	FM-100[d]	Rayleigh[e] match
Inactivating mutation deutans	6643	49.75	51.84	1	1	W → Stop Codon at AA #149	>0.081	Deutan 8.5 d.c. 3.97	Not done	Match all
	110[a]	48.87	52.09	1	1	LIAVA	>0.081	Deutan 9.5 d.c. 4.24	Not done	Match all
Single-gene deutans	3503	106.10	0	1	0	N/A	>0.081	Not done	256	Match all
	3507	106.29	0	1	0	N/A	>0.081	Not done	210	0–39
	3511	105.38	0	1	0	N/A	>0.081	Not done	Not done	Not done
	3513	105.42	0	1	0	N/A	>0.081	Not done	203	Not done
	6760	101.18	0	1	0	N/A	>0.081	Deutan 9.5 d.c. 4.33	Not done	Match all
Multiple-gene deutans	400	39.05	69.63	2	2	None	0.051	Deutan 2 d.c. 1.52	Not done	23–35
	433	69.52	70.37	2	1	None	>0.081	Deutan 9 d.c. 3.90	174	Match all
	3509	68.07	64.35	2	1	None	>0.081	Not done	282	Not done
	6537	105.5	51.05	2	0	N/A	0.022	0 d.c. 1.12	Not done	15–19

[a] This subject was previously reported and described by (Carroll et al., 2004; Neitz et al., 2004).
[b] *D* values are reported, indicating the most difficult plate read by the subject. The *D* value is represents the chromaticity difference between the symbol and the background. The greater the *D* value, the worse the discrimination. (Neitz, Neitz, & Kainz, 1996).
[c] Lanthony's Desaturated D15; average number of diametrical crossings and average color confusion index are reported from two administrations. (Lanthony, 1978).
[d] Average total error score from two administrations. Normal total error score is 50 ± 15 (30–39 year old) and 68 ± 16 (40–49 year old) (Kinnear & Sahraie, 2002).
[e] Limits of the match range on a Model 1 Nagel Anomaloscope. Normal is around 40, with a match range of 3–5 Nagel units.

Fig. 1. DNA sequence electropherograms showing nucleotide positions 937 through 943 in exon 3 from a color-normal male (*top*) and from deutan male subject 6643 (*bottom*). In the subject 6643 a substitution at nucleotide position 940 changes codon 149 from TGG encoding the amino acid tryptophan to TAG which is a signal to terminate translation.

1.25° eccentricity are shown for the three main sub-groups and for subject 6643 (Fig. 3A–E). For the Voronoi analysis, each cone was identified, labeled (Fig. 3F–J) and a polygon was created based on the points (cones) in a 2D plane that are equidistant between that cone and each of its nearest neighbors, as illustrated by representative images in Fig. 3K–O. Assessment of the cone mosaic organization uses metrics derived from the Voronoi domains. Retinal mosaics are typically organized hexagonally, with each cone neighbored by an average of six cones, represented by a six-sided polygon. In disrupted mosaics this organization is altered and both the percentage of cones with six neighbors and the standard deviation of the average number of neighboring cones assess this degree of disruption. Qualitatively, the regularity of the mosaic harboring the nonsense mutation (Fig. 3N) is similar to the mosaics from both multiple- and single-gene deutans as well as normal trichromats (Fig. 3K–M). In contrast, the regularity of the mosaic harboring the LIAVA deleterious combination has significant disruptions. A quantitative assessment confirms this observation. Comparison of the percentage of cones with six-sided Voronoi domains for normal trichromats, multiple-gene deutans, single-gene deutans and subject 6643 revealed no significant differences. As there was also no difference in cone density, all three groups were combined to represent normal mosaic regularity in this analysis. Fig. 4 demonstrates the result of this analysis at 1.0° retinal eccentricity.

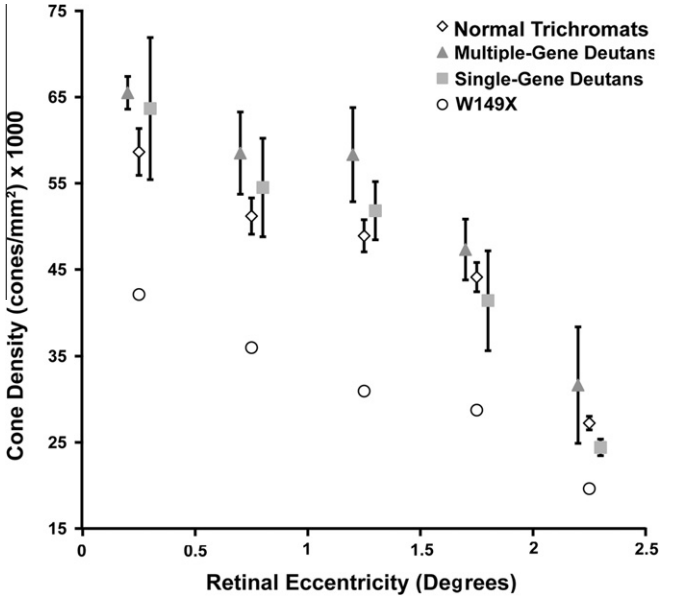

Fig. 2. Mean cone densities for normal trichromats (*diamonds*), single-gene deutans (*squares*) and multi-gene deutans (*triangles*) at each of five retinal eccentricities (0.5°, 0.75°, 1.0°, 1.25° and 2.5°). For comparison, the cone densities at each of these locations for subject 6643 with the W149X mutation shown (*circles*). For each of the mean density values, error bars are gives to show ±1 SEM. Symbols are displaced horizontally for easier visualization. For data points in which no error bars are visible, they are contained entirely within the symbol. Multiple-gene and single-gene deutans did not differ significantly from normals ($p > 0.08$ at all locations, Mann–Whitney test). A Z-score analysis revealed a significant reduction in cone density for subject 6643 with the W149X mutation compared to normal trichromats with p values as follows: 0.5°, $p = 0.062$; 0.75°, $p = 0.027$; 1.0°, $p = 0.016$; 1.25°, $p = 0.029$; 2.5°, $p = 0.015$.

The retinal mosaics of the normal and colorblind controls demonstrated variable regularity, with 47–75% of cones in these mosaics having six-sided Voronoi domains, this is consistent with previous estimates (Baraas et al., 2007; Carroll et al., 2010; Li & Roorda, 2007). No significant difference in regularity was found between the normal retinas and the W149X retina, with 43–53% of the cones in the W149X retina possessing six-sided Voronoi domains ($p = 0.11$).

4. Discussion

Here we provide direct evidence that there is no difference in cone density or mosaic regularity in the central retina between normal trichromats and either multiple-gene or single-gene deutans. These results are consistent with previous studies employing a variety of techniques to evaluate cone density in color vision deficiency versus normal trichromacy (Berendschot, van de Kraats, & van Norren, 1996; Carroll et al., 2004, 2009; Cicerone & Nerger, 1989; Kremers, Usui, Scholl, & Sharpe, 1999; Wesner, Pokorny, Shevell, & Smith, 1991). Our finding that single-gene deutans had similar cone density as individuals with multiple genes (either red–green defective or color-normal) supports the current stochastic model of L/M-gene expression (Smallwood et al., 2002).

It is expected that the W149X mutant M-opsin gene will be transcribed; however, the resulting mRNA transcript will have a translation termination signal that is 537 nucleotides upstream of the last (3′-most) exon/exon junction. The mRNA is thus likely to be degraded by the nonsense mediated decay pathway and the cones are unlikely to contain any opsin (Nagy & Maquat, 1998). In cones expressing a gene encoding the C203R mutation, a mutant opsin may be produced but it is likely retained in the endoplasmic reticulum (Kazmi, Sakmar, & Ostrer, 1997; Mendes, van der Spuy, Chapple, & Cheetham, 2005); in contrast, cones expressing a gene encoding the LIAVA polymorphism are expected to contain the mutant opsin protein (Carroll et al., 2004; Crognale et al., 2004). Previously published adaptive optics images (see Fig. 3) from the retina of a subject whose color vision deficiency is caused by the LIAVA deleterious combination revealed intermittent dark areas, equal in size to one or more cones, where no cones were visible by adaptive optics (Carroll et al., 2004). The authors hypothesized these dark areas represented the loci at which cones

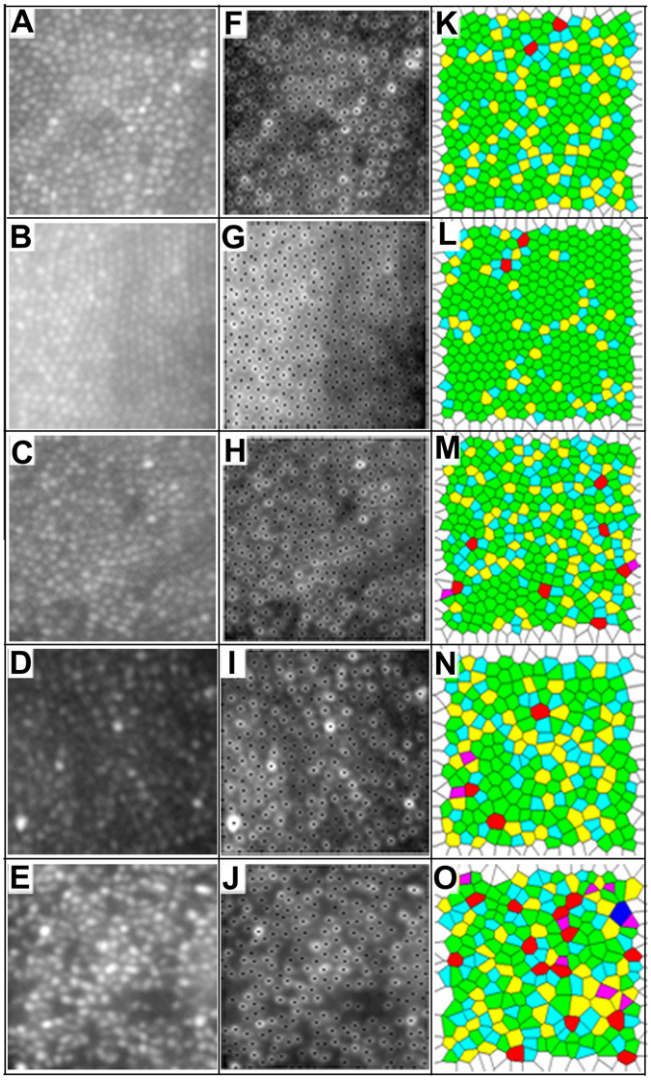

Fig. 3. Cone mosaic regularity assessment using Voronoi domain analysis. The left column shows representative adaptive optics images taken from approximately 1.25° eccentricity in a representative trichromat (subject 3501) (*A*), a representative multiple-gene deutan (subject 400) (*B*), a representative single-gene deutan (subject 3503) (*C*), subject 6643 with the nonsense mutation (*D*), and subject with the LIAVA polymorphism (*E*). Shown in the middle column are the same retinal images from the left column with each individual cone location labeled, *F* is the normal trichromat, *G* is the multiple-gene deutan, *H* is the single-gene deutan, *I* is subject 6643, and *J* is the subject with the LIAVA polymorphism. The right column displays the Voronoi domains associated with each cone identified in the normal trichromat (*K*), the multiple-gene deutan (*L*), the single-gene deutan (*M*), subject 6643 (*N*), and the subject with the LIAVA polymorphism (*O*). The colors in *K*–*O* indicate the number of sides for each Voronoi domain (magenta = 4, cyan = 5, green = 6, yellow = 7, and red = 8). Retinal mosaics are typically organized triangularly; therefore large areas of green (six-sided) domains indicate a regularly organized mosaic. Areas with other colors denote regions where there is a disruption in the triangular packing of the mosaic.

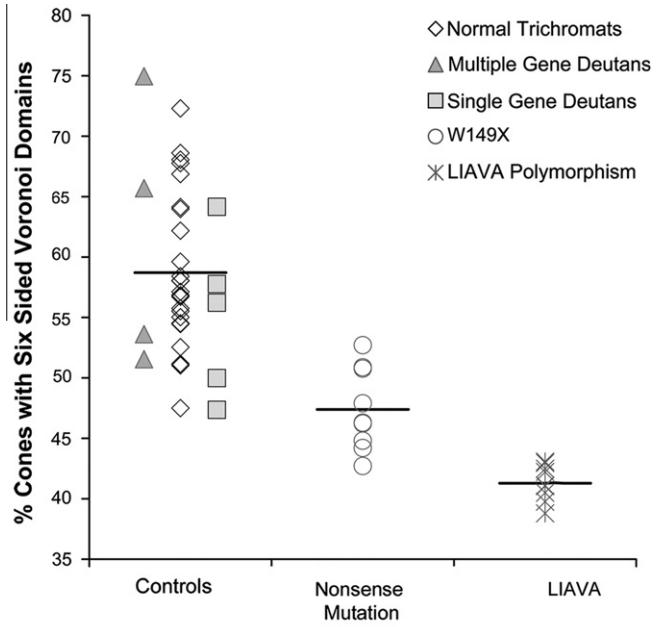

Fig. 4. Quantitative assessment of mosaic regularity. This graph shows the percentage of cones that have six-sided Voronoi domains in the normal trichromats, multiple-gene deutans, single-gene deutans, the nonsense mutation subject, and a previously reported LIAVA subject. As no significant difference was found in density or regularity between the normal trichomats, multiple-gene deutans, and single-gene deutans, they were combined as one group of controls for this comparison. Individual data points for the normal controls represent individual retinas at 1° eccentricity (trichromats, $n = 24$; multiple-gene deutans, $n = 4$; single-gene deutans, $n = 3$; total, $n = 33$). Individual data points for the two subjects with inactivating mutations represent measurements at nine different points within the same retina, also at 1° eccentricity. Horizontal bars represent either the mean value for the entire group of controls (normal trichromats plus multiple-gene and single-gene deutans, $n = 33$) or the mean value for each subject with an inactivating mutation (nonsense mutation, $n = 9$; LIAVA, $n = 9$).

expressing the LIAVA pigment had been structurally compromised, *i.e.* there is no outer segment or a malformed outer segment (Carroll et al., 2004). Thus, for the LIAVA mutation, imaging results suggest that although cone function is completely compromised, photoreceptor cell viability may not be. By comparison, adaptive optics images from individuals with the C203R mutation revealed mosaics of reduced density, but that were regularly packed (Carroll et al., 2009). It was hypothesized that the C203R mosaics were regularly packed because the cells expressing the C203R pigment degenerated early in foveal development due to an absence of opsin in the outer segment. In this case it is thought that the post-natal packing of cones "rescued" the regularity of the remaining cones in the mosaic (Carroll et al., 2009). Here, we found that the W149X opsin mutation was associated with significantly reduced cone density but no disruption in cone packing compared to controls. This suggests that cones expressing the W149X mutation have a similar fate as those expressing the C203R mutation. The average reduction in cone density (32%) in the W149X retina is consistent with a loss of the M-cone submosaic in this individual because on average M cones represent about 30% of the total L/M cone population in a normal trichromat (Carroll, Neitz, & Neitz, 2002; Hofer, Carroll, Neitz, Neitz, & Williams, 2005; Rushton & Baker, 1964).

The model emerging from our work is that the timing and severity of cone mosaic disruptions in individuals with cone opsin mutations will depend upon the specific mutation and the relative proportion of cones expressing the mutant opsin. Given the enormous variability in "normal" L:M cone ratio (Carroll et al., 2002; Hofer et al., 2005; Rushton & Baker, 1964), it is possible that in some individuals as many as 90% of their L/M cones express the mutant opsin and are non-functional.[1] Whether in these instances there is a more pronounced retinal phenotype, remains to be seen. However there are several reports in the literature in which red–green color vision deficiency is associated with a retinal dystrophy (Kellner, Sadowski, Zrenner, & Foerster, 1995; Michaelides et al., 2005; Reichel, Bruce, Sandberg, & Berson, 1989; Scholl, Kremers, Besch, Zrenner, & Jägle, 2006; Scholl, Kremers, & Wissinger, 2001). It is tempting to speculate that some of these cases may indeed represent instances where a mutant opsin was expressed in such a large number of cones that it affected the overall health of the retina. Continued work combining molecular genetic analysis and high-resolution retinal imaging will help further refine our understanding of the deleterious nature of red–green color vision defects.

Acknowledgments

JC is the recipient of a Career Development Award from Research to Prevent Blindness. This study was supported by NIH Grants P30EY001931, P30EY001319, R01EY017607, R01EY009303, R01EY009620, R01EY004367, Fight for Sight, Harry J. Heeb Foundation, Hope for Vision, Gene and Ruth Posner Foundation, The E. Matilda Ziegler Foundation for the Blind, RD and Linda Peters Foundation, and unrestricted departmental grants from Research to Prevent Blindness (Medical College of Wisconsin & University of Rochester). The authors thank D. Conklyn, K. Stepien, C. Siebe, C. Sloan, P.M. Summerfelt, and S. Thompson for technical assistance. This investigation was conducted in a facility constructed with support from Research Facilities Improvement Program Grant Number C06 RR-RR016511 from the National Center for Research Resources, National Institutes of Health.

Appendix A. Supplementary material

Supplementary data associated with this article can be found, in the online version, at doi:10.1016/j.visres.2010.09.015.

References

Baraas, R. C., Carroll, J., Gunther, K. L., Chung, M., Williams, D. R., Foster, D. H., et al. (2007). Adaptive optics retinal imaging reveals S-cone dystrophy in tritan color-vision deficiency. *Journal of the Optical Society of America A, 24*(5), 1438–1446.

Berendschot, T. T., van de Kraats, J., & van Norren, D. (1996). Foveal cone mosaic and visual pigment density in dichromats. *Journal of Physiology (London), 492*, 307–314.

Bollinger, K., Bialozynski, C., Neitz, J., & Neitz, M. (2001). The importance of deleterious mutations of M pigment genes as a cause of color vision defects. *Color Research and Application, 26*, S100–S105.

Bollinger, K., Sjoberg, S. A., Neitz, M., & Neitz, J. (2004). Topographical cone photopigment in deutan-type red–green color gene expression vision defects. *Vision Research, 44*(2), 135–145.

Carroll, J., Baraas, R. C., Wagner-Schuman, M., Rha, J., Siebe, C. A., Sloan, C., et al. (2009). Cone photoreceptor mosaic disruption associated with Cys203Arg mutation in the M-cone opsin. *Proceedings of the National Academy of Sciences USA, 106*(49), 20948–20953.

Carroll, J., Neitz, M., Hofer, H., Neitz, J., & Williams, D. R. (2004). Functional photoreceptor loss revealed with adaptive optics: An alternate cause for color blindness. *Proceedings of the National Academy of Sciences USA, 101*(22), 8461–8466.

Carroll, J., Neitz, M., & Neitz, J. (2002). Estimates of L:M cone ratio from ERG flicker photometry and genetics. *Journal of Vision, 2*(8), 531–542.

Carroll, J., Rossi, E. A., Porter, J., Neitz, J., Roorda, A., Williams, D., et al. (2010). Deletion of the X-linked opsin gene array locus control region (LCR) results in disruption of the cone mosaic. *Vision Research, 50*, 1989–1999.

Chui, T. Y. P., Song, H. X., & Burns, S. A. (2008). Individual variations in human cone photoreceptor packing density: Variations with refractive error. *Investigative Ophthalmology and Visual Science, 49*(10), 4679–4687.

[1] The L/M-cone submosaic comprises about 95% of the total cone population. Thus a loss of 90% of the L/M cones would represent about an 85% loss in total cone number, which could have quite different consequences for the remaining rod and cone mosaic than perhaps a 5% loss of cones.

Cicerone, C. M., & Nerger, J. L. (1989). The density of cones in the fovea centralis of the human dichromat. *Vision Research, 29*(11), 1587–1595.

Crognale, M. A., Fry, M., Highsmith, J., Haegerstrom-Portnoy, G., Neitz, M., Neitz, J., et al. (2004). Characterization of a novel form of X-linked incomplete achromatopsia. *Visual Neuroscience, 21*, 197–203.

Curcio, C. A., Sloan, K. R., Kalina, R. E., & Hendrickson, A. E. (1990). Human photoreceptor topography. *The Journal of Comparative Neurology, 292*, 497–523.

Deeb, S. S., Lindsey, D. T., Hibiya, Y., Sanocki, E., Winderickx, J., Teller, D. Y., et al. (1992). Genotype–phenotype relationships in human red/green color-vision defects: Molecular and psychophysical studies. *American Journal of Human Genetics, 51*, 687–700.

Drummond-Borg, M., Deeb, S. S., & Motolsky, A. G. (1989). Molecular patterns of X chromosome-linked color vision genes among 134 men of European ancestry. *Proceedings of the National Academy of Sciences USA, 86*, 983–987.

Duncan, J. L., Zhang, Y., Gandhi, J., Nakanishi, C., Othman, M., Branham, K. E., et al. (2007). High-resolution imaging with adaptive optics in patients with inherited retinal degeneration. *Investigative Ophthalmology and Visual Science, 48*(7), 3283–3291.

Gardner, J. C., Webb, T. R., Kanuga, N., Robson, A. G., Holder, G. E., Stockman, A., et al. (2010). X-linked cone dystrophy caused by mutation of the red and green cone opsins. *American Journal of Human Genetics, 87*(1), 26–39.

Hayashi, T., Motulsky, A. G., & Deeb, S. S. (1999). Position of a 'green–red' hybrid gene in the visual pigment array determines colour-vision phenotype. *Nature Genetics, 22*(May), 90–93.

Hofer, H., Carroll, J., Neitz, J., Neitz, M., & Williams, D. R. (2005). Organization of the human trichromatic cone mosaic. *The Journal of Neuroscience, 25*(42), 9669–9679.

Hofer, H., Chen, L., Yoon, G. Y., Singer, B., Yamauchi, Y., & Williams, D. R. (2001). Improvement in retinal image quality with dynamic correction of the eye's aberrations. *Optics Express, 8*(11), 631–643.

Jagla, W. M., Jägle, H., Hayashi, T., Sharpe, L. T., & Deeb, S. S. (2002). The molecular basis of dichromatic color vision in males with multiple red and green visual pigment genes. *Human Molecular Genetics, 11*, 23–32.

Kazmi, M. A., Sakmar, T. P., & Ostrer, H. (1997). Mutation of a conserved cysteine in the X-linked cone opsins causes color vision deficiencies by disrupting protein folding and stability. *Investigative Ophthalmology and Visual Science, 38*(6), 1074–1081.

Kellner, U., Sadowski, B., Zrenner, E., & Foerster, M. H. (1995). Selective cone dystrophy with protan genotype. *Investigative Ophthalmology and Visual Science, 36*(12), 2381–2387.

Kinnear, P. R., & Sahraie, A. (2002). New Farnsworth-Munsell 100 hue test norms of normal observers for each year of age 5–22 and for decades 30–70. *British Journal of Ophthalmology, 86*(12), 1408–1411.

Kremers, J., Usui, T., Scholl, H. P. N., & Sharpe, L. T. (1999). Cone signal contributions to electrograms [electroretinograms] in dichromats and trichromats. *Investigative Ophthalmology and Visual Science, 40*(5), 920–930.

Lanthony, P. (1978). The desaturated panel D-15. *Documenta Ophthalmologica, 46*, 185–189.

Li, K. Y., Tiruveedhula, P., & Roorda, A. (2010). Inter-subject variability of foveal cone photoreceptor density in relation to eye length. *Investigative Ophthalmology and Visual Science* (published online ahead of print August 4, 2010).

Li, K. Y., & Roorda, A. (2007). Automated identification of cone photoreceptors in adaptive optics retinal images. *Journal of the Optical Society of America A, 24*(5), 1358–1363.

McClements, M. E., Neitz, M., Moore, A. T., & Hunt, D. M. (2010). Bornholm eye disease arises from a specific combination of amino acid changes encoded by exon 3 of the L/M cone opsin gene. Investigative Ophthalmology and Visual Science, 51, ARVO E-Abstract 2609.

Mendes, H. F., van der Spuy, J., Chapple, J. P., & Cheetham, M. E. (2005). Mechanisms of cell death in rhodopsin retinitis pigmentosa: Implications for therapy. *Trends in Molecular Medicine, 11*(4), 177–185.

Michaelides, M., Johnson, S., Bradshaw, K., Holder, G. E., Simunovic, M. P., Mollon, J. D., et al. (2005). X-linked cone dysfunction syndrome with myopia and protanopia. *Ophthalmology, 112*(8), 1448–1454.

Mizrahi-Meissonnier, L., Merin, S., Banin, E., & Sharon, D. (2010). Variable retinal phenotypes caused by mutations in the X-linked photopigment gene array. *Investigative Ophthalmology and Visual Science, 51*(8), 3884–3892.

Nagy, E., & Maquat, L. E. (1998). A rule for termination-codon position within intron-containing genes; when nonsense affects RNA abundance. *Trends in Biochemical Sciences, 23*(6), 198–199.

Nathans, J., Maumenee, I. A., Zrenner, E., Sadowski, B., Sharpe, L. T., Lewis, R. A., et al. (1993). Genetic heterogeneity among blue-cone monochromats. *American Journal of Human Genetics, 53*, 987–1000.

Nathans, J., Thomas, D., & Hogness, D. S. (1986). Molecular genetics of human color vision: The genes encoding blue, green, and red pigments. *Science, 232*, 193–202.

Neitz, M., Bollinger, K., & Neitz, J. (2003). Middle wavelength sensitive photopigment gene expression is absent in deuteranomalous colour vision. In J. D. Mollon, J. Pokorny, & K. Knoblauch (Eds.), *Normal & defective colour vision* (pp. 318–327). New York: Oxford University Press.

Neitz, M., Carroll, J., Renner, A., Knau, H., Werner, J. S., & Neitz, J. (2004). Variety of genotypes in males diagnosed as dichromatic on a conventional clinical anomaloscope. *Visual Neuroscience, 21*, 205–216.

Neitz, M., & Neitz, J. (2001). A new mass screening test for color-vision deficiencies in children. *Color Research and Application, 26*, S239–S249.

Neitz, J., Neitz, M., & Kainz, P. M. (1996). Visual pigment gene structure and the severity of color vision defects. *Science, 274*(5288), 801–804.

Putnam, N. M., Hofer, H. J., Doble, N., Chen, L., Carroll, J., & Williams, D. R. (2005). The locus of fixation and the foveal cone mosaic. *Journal of Vision, 5*(7), 632–639.

Reichel, E., Bruce, A. M., Sandberg, M. A., & Berson, E. L. (1989). An electroretinographic and molecular genetic study of X-linked cone degeneration. *American Journal of Ophthalmology, 108*, 540–547.

Rha, J., Schroeder, B., Godara, P., & Carroll, J. (2009). Variable optical activation of human cone photoreceptors visualized using short coherence light source. *Optics Letters, 34*(24), 3782–3784.

Rushton, W. A. H., & Baker, H. D. (1964). Red/green sensitivity in normal vision. *Vision Research, 4*, 75–85.

Scholl, H. P. N., Kremers, J., Besch, D., Zrenner, E., & Jägle, H. (2006). Progressive cone dystrophy with deutan genotype and phenotype. *Graefe's Archive for Clinical and Experimental Ophthalmology, 244*(2), 183–191.

Scholl, H. P. N., Kremers, J., & Wissinger, B. (2001). Macular dystrophy with protan genotype and phenotype studied with cone type specific ERG's. *Current Eye Research, 22*(3), 221–228.

Sharpe, L. T., Stockman, A., Jägle, H., Knau, H., Klausen, G., Reitner, A., et al. (1998). Red, green, and red–green hybrid pigments in the human retina: Correlations between deduced protein sequences and psychophysically measured spectral sensitivities. *The Journal of Neuroscience, 18*, 10053–10069.

Silva, A. L., & Romano, L. (2009). The mammalian nonsense-mediated mRNA decay pathway: To decay or not to decay! Which players make the decision? *Federation of European Biochemical Societies Letters, 583*(3), 499–505.

Smallwood, P. M., Wang, Y. S., & Nathans, J. (2002). Role of a locus control region in the mutually exclusive expression of human red and green cone pigment genes. *Proceedings of the National Academy of Sciences USA, 99*(2), 1008–1011.

Torti, C., Považay, B., Hofer, B., Unterhuber, A., Carroll, J., Ahnelt, P. K., et al. (2009). Adaptive optics optical coherence tomography at 120, 000 depth scans/s for non-invasive cellular phenotyping of the living human retina. *Optics Express, 17*(22), 19382–19400.

Ueyama, H., Kuwayama, S., Imai, H., Oda, S., Nishida, Y., Tanabe, S., et al. (2004). Analysis of L-cone/M-cone visual pigment gene arrays in Japanese males with protan color-vision deficiency. *Vision Research, 44*(19), 2241–2252.

Ueyama, H., Kuwayama, S., Imai, H., Tanabe, S., Oda, S., Nishida, S., et al. (2002). Novel missense mutations in red/green opsin genes in congenital color-vision deficiencies. *Biochemical and Biophysical Research Communications, 294*, 205–209.

Wesner, M. F., Pokorny, J., Shevell, S. K., & Smith, V. C. (1991). Foveal cone detection statistics in color-normals and dichromats. *Vision Research, 31*(6), 1021–1037.

Winderickx, J., Sanocki, E., Lindsey, D. T., Teller, D. Y., Motulsky, A. G., & Deeb, S. S. (1992). Defective colour vision associated with a missense mutation in the human green visual pigment gene. *Nature Genetics, 1*, 251–256.

Wissinger, B., Papke, M., Tippmann, S., & Kohl, S. (2006). Genotypes in blue cone monochromacy. Investigative Ophthalmology and Visual Science, 47, ARVO E-Abstract 4609.